SMASIS2012-8096

DUAL MODE SENSING OF CRACK GROWTH IN STEEL BRIDGE STRUCTURES

Lingyu Yu, Assistant Professor

Mechanical Engineering Department, University of South Carolina

Columbia, SC 29208, yu3@cec.sc.edu

Liuxian Zhao, PhD Student

Mechanical Engineering Department, University of South Carolina

Columbia, SC 29208, zhao56@email.sc.edu

Zhenhua Tian, PhD Student

Mechanical Engineering Department, University of South Carolina

Columbia, SC 29208, tianz@email.sc.edu

Victor Giurgiutiu, Professor

Mechanical Engineering Department, University of South Carolina

Columbia, SC 29208, giurgiut@cec.sc.edu

Paul Ziehl, Associate Professor

Civil and Environmental Engineering Department, University of South Carolina

Columbia, SC 29208, ziehl@cec.sc.edu

ABSTRACT

Monitoring of fatigue cracking in steel bridge structures using a combined passive and active scheme has been approached by the authors. Passive acoustic emission (AE) monitoring is able to detect crack growth behavior by picking up the stress waves resulting from the breathing of cracks while active ultrasonic pulsing can quantitatively assess structural defect by sensing out an interrogating pulse and receiving the structural reflections. The dual-mode sensing functionality is pursued by using the R15I ultrasonic transducers.

In the paper, we presented the subject dual-mode sensing on steel compact tension (CT) specimens in a laboratory setup. Passive AE sensing was performed during fatigue loading and showed its capability to detect crack growth and location. At selected intervals of loading cycles, the test was paused to allow for active sensing by pulsing the transducers in a round-robin pattern. Plate waves were excited, propagated and interacted within the structure. Several approaches were proposed to analyze the interrogation data and to correlate the data features with crack growth. Root means square deviation (RMSD) damage index (DI) was found as a good indicator for indicating the overall crack development. Short time Fourier transform (STFT) provided both time and frequency information at the same time. Moreover, wave velocity analysis showed interesting results when crack developed across the transmitter-receiver path.

1 INTRODUCTION

Bridge structures throughout United States are being used for many years and call for the implementation of a continuous monitoring system that can detect the damage timely and extend their service life. Cracks and flaws in steel bridge structures may originate from their fabrication process and grow because of fatigue and corrosion (Pullin et al, 2008). What is more, the inventory of car in America is 46 million in 1997 while the number increased to 250 million in 2011 which leads to the steel bridges work overloaded and results in decreasing of their life span. The unpredictability of the degradation process needs timely inspection and evaluation of these structures in order to repair and replace the damaged components. Among various inspection techniques, structural health monitoring (SHM) is an emerging technology which

Copyright © 2012 by ASME

deals with the development and implementation of techniques and systems where monitoring, inspection and damage detection become an integral part of the structure. It further merges a variety of techniques related to the diagnostics and prognostics (Naie and Cai, 2010) (Shiotani et al, 2007).

Active or growing flaw such as cracking and corrosion emits acoustic emission (AE) waves under load. AE waves are stress waves that arise from the rapid release of strain energy that follows micro structural changes in a material (Vahaviolos, 1996). AE waves can be recorded by means of transducers placed on the surface of a structure. Analysis of these recorded signals provides information about the source of the AE with very high sensitivity. It is classified as passive structural health monitoring techniques and can be used for real time monitoring (Tan et al, 2009). The "active" ultrasonic SHM approach, on the other hand, uses an artificially generated source signal and a receiver to interrogate the damage that exists in the structure. Figure 1 illustrates the "passive" and "active" concepts in NDT (Grosse and Ohtsu, 2008).
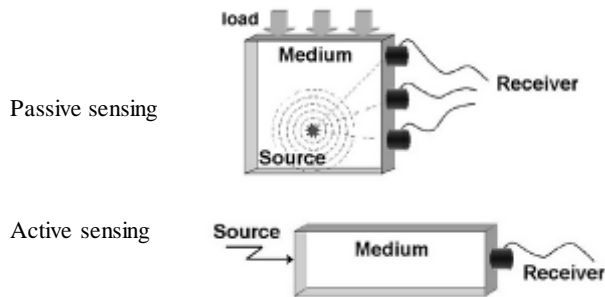

Figure 1   Passive and active sensing in NDE/SHM (Grosse and Ohtsu, 2008)

The research presented in this paper is sponsored by National Institute of Standards and Technology (NIST) the Technology Innovation Program (TIP), which incorporates novel and promising sensing approaches together with energy harvesting devices to reduce the dramatic uncertainty inherent into any bridge inspection and maintenance plan (Yu et al, 2010). One of the challenges in this research is focused on the use of dual mode sensing combing passive and active sensing capabilities to provide information related to the degradation state of the structure and its correlation to a global performance index. The combined schematic is to use acoustic emission to detect the presence of fatigue cracks in steel bridges in their early stage since methods such as ultrasonic is unable to quantify the initial condition of crack growth since most of the fatigue life for these details is consumed while the fatigue crack is too small to be detected. After the crack is present, active pulsing is activated to allow for further quantification of cracks in the absence of dynamic crack growth, which complements AE sensing that relies on damage progression for quantification. The integration of passive AE detection with active sensing will be a technological leap forward from the current practice of periodic and subjective visual inspection, and bridge

management based primarily on history of past performance. The combination of different sensing techniques is realistically envisioned to greatly improve the reliability of damage detection, and provide the reward of optimized decision-making.

2   R15I DULE MODE TRANSDUCER

R15I is a widely used AE transducer. It represents a significant advancement for the field of AE by enclosing a low-noise 40 dB pre-amplifier inside a standard high sensitivity transducer, as shown in Figure 2. These rugged, small size integrated AE transducers eliminate the need for cumbersome pre-amplifiers by incorporating two functions into one, thereby reducing equipment costs and decreasing set-up time for field applications. The R15I transducers are resonant type transducers with a resonant frequency at 150 kHz, providing a good mix of high sensitivity and noise rejection. They have proven very useful for monitoring common structures such as pipelines, vessels, bridges, and storage tanks in petroleum, refineries, chemical plants, offshore platforms, as well as factory and process monitoring applications. A typical AE signal captured during fatigue loading on a 19 mm thick steel plate is shown in Figure 3 (a).

Figure 2   Configuration of R15I transducer

R15I also comes with an optional "auto sensor test" (AST) capability to allow the AE sensor sending out a simulated AE wave. Therefore, it allows for any AE channel to pulse the transducer, while the receiving electronics remains active for recording, thereby giving feedback of the conditions of transducers themselves. Hence, a R15I transducer with AST function can "pulse" like an ultrasonic actuator to send out an interrogation signal that other transducers can detect. A sample AST signal received by a R15I transducer 140 mm away from the pulsing R15I is shown in Figure 3 (b).

2   Copyright © 2012 by ASME
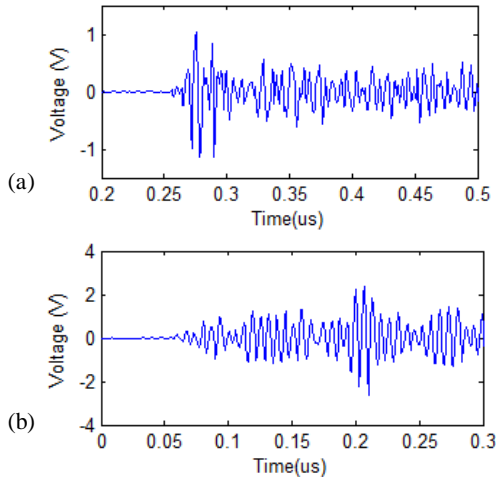
Figure 3   Dual mode passive AE sensing and active sensing of R15I transducer. (a) An AE signal due to cracking recorded during a fatigue loading test; (b) an "active" signal received in the R15I AST test

3   R15I PASSIVE AE SENSING TESTS

A 19 mm thick compact Tension (CT) specimen made of structural steel A572 grade 50 was used in this study. The geometry of the specimen is displayed in Figure 4. Custom fixtures were designed and fabricated to mount the CT specimen. Cyclic tension loads of minimum 1 KN and maximum 50 KN were applied to the specimen using servo hydraulic mechanical testing machine (810 Material Test System). Fatigue tests were conducted under load-controlled mode with frequency of 1 HZ. A clip gage was employed to measure the crack mouth opening displacement (CMOD) to clarify crack opening and closure and to determine the magnitude of the CMOD. The surface cracks were also monitored optically with a high resolution recording microscope. Two different pre-amplifiers, one with the band pass filter in the range of 100-200 kHz and the other with wideband BP-SYS, have been used.
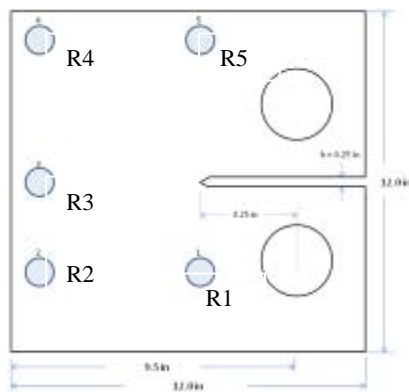

Figure 4   AE detection on a 19 mm CT specimen, geometry of the specimen and arrangement of transducers;

The crack localization analyzed by PAC AEwin software during CT testing is shown in Figure 5. With R15I, 1171 AE

events were detected before the final failure. Figure 5(a) gives the cumulative acoustic energy of R15I and PWA together with the crack opening displacement. Figure 5(b) is the crack detection and localization when the crack size reaches 0.83 mm. It should be noted that the localization algorithm in the PAC AE localization software was not optimized for this specimen (Yu et al, 2012).
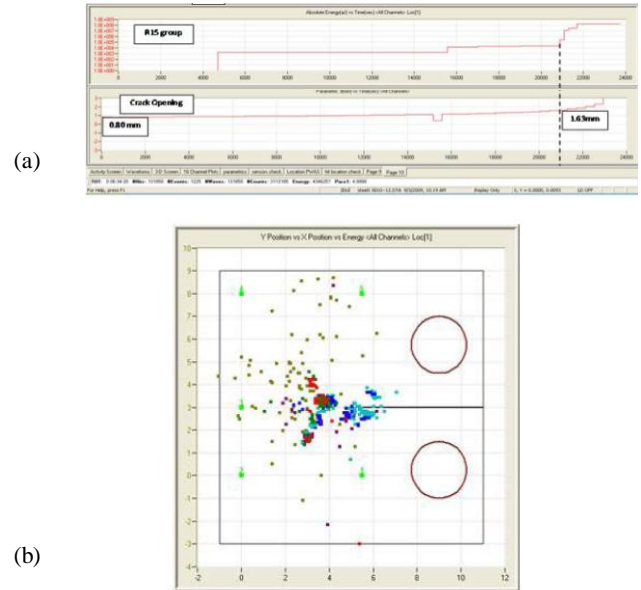

Figure 5   Crack localization in CT test on 19 mm steel specimen. (a) Cumulative acoustic energy by R15I; (b) cracking detection and localization by R15I (Yu et al 2012)

4   R15I ACTIVE SENSING TESTS

With the AST capability, it allows the AE system to control a pulser that is integral to PAC AST equipped preamplifiers and the integral preamplifier sensors. In this section, we explored the potential of using R15I as active transducer to monitor the crack formation and growth during CT testing.

4.1   EXPERIMENTAL SETUP

The 19 mm CT test specimen was used in the active sensing study. Note the initial notch on the specimen is about 82.6 mm measured from the load line. Five R15I have been installed on the front surface with the same layout as used in passive sensing. The setup of the specimens is displayed in Figure 6. CT test has been performed using MTS machine to cause the crack growth along the pre-notch. A total of 13 crack sizes were measured as given in Table 1. At each crack size, an active AST test was performed between all transducers in a round robin pattern. For example, transducer R1 was pulsed 5 times with a pulse width of 10 μs and a pulse interval of 1 s. The pulsing excited plate waves propagating in all directions in the structure. When arriving at another R15I transducer, the signal starts to be recorded after it reaches the data acquisition threshold of the DiSP system. The recording time is known as

3   Copyright © 2012 by ASME

the *delta t* information during the data acquisition process. Both waveforms and *delta t* together with other related information are saved by the system. The corresponding *delta t* values are provided in Table 1. Several signals at different crack length were plotted in Figure 7.
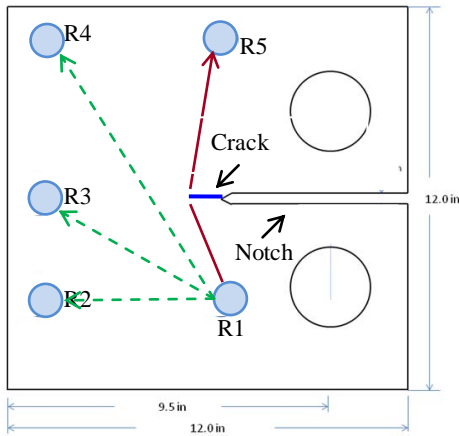

Figure 6   R15I active sensing layout

Table 1 The increment of the crack size by MTS machine

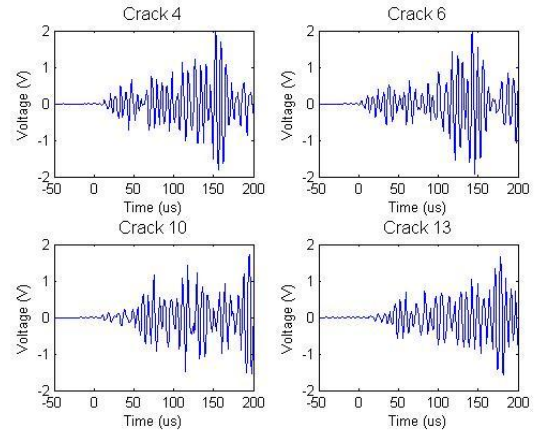| Crack No.	Crack Extension (mm)	*delta T* (µs)
0	0	51
1	1.0	47
2	3.6	48
3	5.7	47
4	8.9	48
5	12.5	48
6	16.1	58
7	20.9	58
8	27.6	59
9	34.3	60
10	58.5	71
11	66.9	73
12	76.6	87
13	85.9	86

Figure 7   Four signals at different crack length. Transducer 1 used as the transmitter and transducer 5 used as the receiver

4.2   INTERPRETATION OF ARRIVAL TIME DIFFERENCE

It has been mentioned that R15I transducer has a built-in 40 dB preamplifier. The relation between the unit of dB and volt is given as:

$$V_{measure} = 10^{\left(\frac{\text{Amp(dB)}}{20} + \text{Preamp(dB)}\right)} V_{ref} \qquad (1)$$

Amp (dB) is the threshold in dB, which is 40 dB in the present measurements. V_{ref} is the reference voltage, which is the voltage at 0 dB (i.e., 10^{-6} V). *Preamp* (dB) is the preamplifier gain which is 40 dB for R15I. According to this equation, the threshold of R15I can be obtained in volt, which is 0.01 V. It means when the signal propagates to the receiver and its magnitude reaches to 0.01 volt, the data acquisition occurs. Several signals were plotted with their zoomed-in view shown in Figure 8 (R1 as the transmitter and R5 as the receiver).
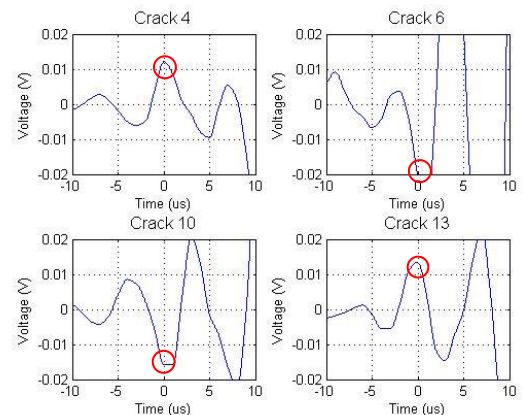

Figure 8   Local amplification of the raw signals. Transducer 1 used as the transmitter and transducer 5 used as the receiver

4   Copyright © 2012 by ASME

It can be seen that the time is labeled zero when R15I transducers begin to record signals. The system records the signal does not consider the distance between transmitter and receiver. Therefore, the signals need to be synchronized according to the arrival time difference recorded by the system. Synchronized signals at different crack length were plotted in Figure 9, as compared to the unsynchronized signals in Figure 7.
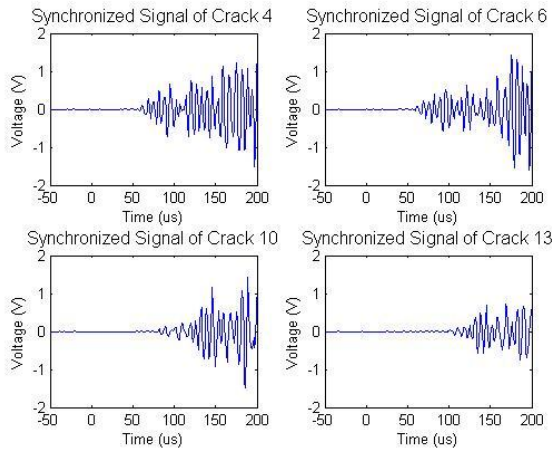

Figure 9   Four synchronized signals at different crack length. Transducer 1 used as the transmitter and transducer 5 used as the receiver

4.3   APPARENT VELOCITY OF WAVE PROPAGATION

During testing of the CT specimen, crack growth was developed from the initial notch. For pulsing-receiving between R1 and R5 (referred as "with crack" pair), this created a diffracted path for wave propagating, as indicated by the solid arrow in Figure 6. That is to say, the wave propagation is from R1 to the crack tip and then from the crack tip to R5. But for others such as those between R1 and R2, R1 and R3, and R1 and R4 (referred as "without crack" pairs) direct wave propagation occurs at most stages of crack development (note that the crack growth stopped before the tip reached the path from R1 to R5), as indicated by the dashed arrows in Figure 6. The path between R1 and R4 will be broken when the crack increases to size #10. We calculated the apparent *velocity of wave propagation* as the ratio between the wave propagation distance and wave propagation time. Wave propagation time is obtained from the data acquisition system using the arrival time *delta t*. The velocity calculated from the without crack pairs in the pristine specimen before the crack development and the velocity calculated from the 'with crack' pair throughout the crack development are plotted in Figure 10(a) and Figure 10(b), respectively.
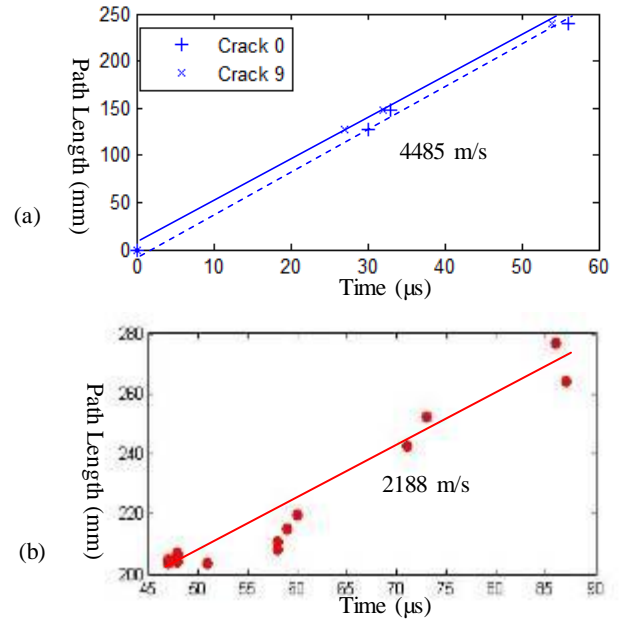

Figure 10   Apparent group velocity plots for various pulser-receiver pairs. (a) Velocity calculated for 'without crack' pairs at pristine condition and at the condition for crack stage #9; (b) velocity calculated for 'with crack pair' starting from the pristine condition and then throughout the 13 crack growth stages

An interesting result can be observed from comparison of Figure 10(a) and Figure 10(b). For 'without crack' pairs, the apparent wave velocity is around 4485 m/s (calculated at pristine and crack No. 9). However, for the 'with crack' pair R1 to R5, the situation is different. In the initial stage, when the crack is very small and the diffraction is negligible, the apparent velocity is also around 4000 m/s. But as the crack increased, the apparent velocity decreased and became approximately 2188 m/s. The comparison of these two situations is plotted in Figure 11. The possible reason for this difference in velocities could be that the diffraction caused by the crack between R1 and R5 decreases the energy arrived at R5, therefore delayed the time when the signal threshold of the DiSP system is passed, thus resulting in a larger *delta t* being recorded. This apparent delay in arrival of the received signal results in a decrease in the calculated apparent velocity.
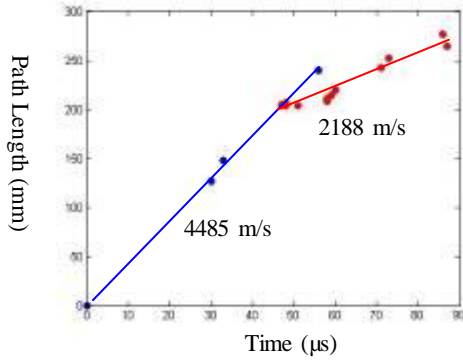
Figure 11 Comparison between the apparent velocity between transducer pairs without crack in their path (4485 m/s) and transducer pairs with crack in their path (2188 m/s)

To have a full understanding of the observed change in the apparent velocity of wave propagation, theoretical wave speed of plate waves in the subject steel plate was derived based on classic Rayleigh-Lamb equation (Rose, 1999). The resulted group velocity curves are given in Figure 12. It is seen that there are four wave modes around R15I's resonant frequency 150 kHz which travel at different group velocities. It is presumed that there are certain wave modes that traveled faster and were strong enough to trigger the data acquisition.
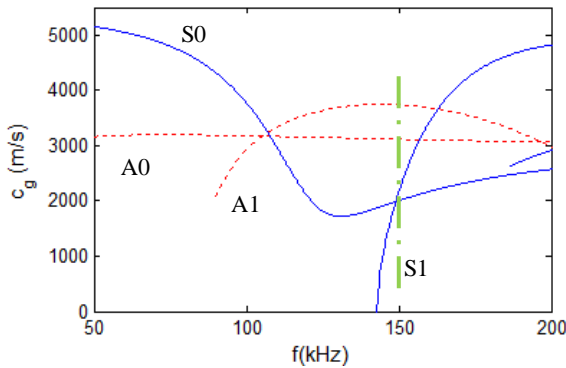

Figure 12 Group velocity of guided waves on a 19-mm steel plate

Hence a digital filtering processing was used to analyze the velocity at various frequency bands. Hanning window was chosen for digital signal filtering. Figure 13(a) is the zoomed-in spectrum plot of a signal received at R5 with R1 as the transmitter. The Original DAQ recorded *delta t* is 51 μs, which indicates that the thresholding and data recording occurred at 51 μs. A Hanning window within the frequency range from 50 kHz to 100 kHz is used for filtering. After using filtering, the new thresholding occurs at 45 μs, as shown in Figure 13(b), triggered earlier than the original signal. It is seen the frequency components within the range from 50 kHz to 100 kHz have higher velocity. It is presumed that when the wave propagation path is broken and interfered by a growing crack, the apparent velocity of wave propagation is decreased since the signal is diffracted by the crack and therefore the wave energy is

scattered in all directions. Only a small fraction of the total wave energy (compared to the unbroken path propagation) can reach the receiver. Additionally, more time is needed for the receiver to record the signals with diffracted path length.
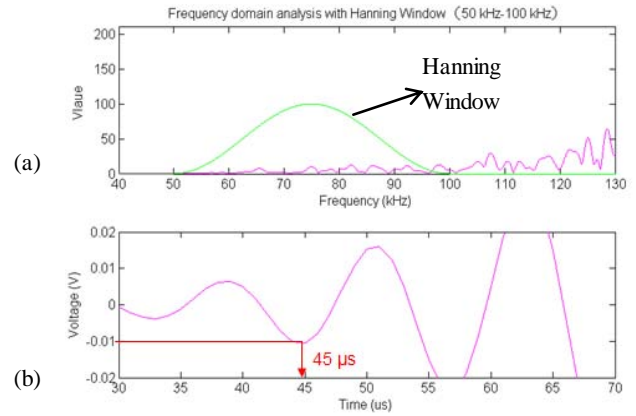

Figure 13 Digital signal filtering design and signal extraction (R1-R5) (crack 0) (a) original signal spectrum and the Hanning window being used for filtering; (b) arrival time of the 50 to 100 kHz frequency component at 45 μs

4.4 WAVEFORM ANALYSIS

4.4.1 Damage index analysis

As waves propagate through a defect, the wave propagation characteristics are modified; hence, analyzing the received waveforms may derive useful information regarding the presence of the defect and/or its development. As a matter of fact, structural health monitoring implicitly includes a process of comparison between a pristine condition and a damage condition. One way to achieve such a comparison is to define a damage index (DI) using root mean square deviation (RMSD) (Yu and Giurgiutiu, 2009). The difference is a good indicator for defect development evaluation since it carries information of both signal amplitude changes and the phase changes. The RMSD DI is defined as:

$$RMSD\ DI = \sqrt{\frac{\sum_{j=0}^{N-1}[s_i(j) - s_0(j)]^2}{\sum_{j=0}^{N-1}s_0^2(j)}} \qquad (2)$$

Where S_i is the ith measurement and S_0 is the baseline signal, and N is the data length.

In our analysis, measurement from crack 1 was used as the baseline. The resulted RMSD DI curve is shown in Figure 14. It can be seen that the DI value increases with the increment of the crack size.
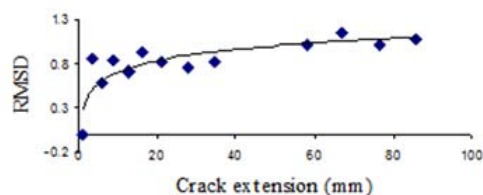
6   Copyright © 2012 by ASME

Figure 14   Damage index analysis of synchronized data

4.4.2 Short-time Fourier transform (STFT) analysis

Due to the non-stationary feature of Lamb wave signals, short-time Fourier transform (STFT) was used to analyze the resulted R15I signals to study how the signals' frequency components evolve with the crack growth. Details of STFT theory can be found in the reference (Cohen, 1995). STFT analysis on selected synchronized R15I data are given in Figure 15. The maximum amplitudes of the signals at each crack are labeled in the figure. It can be seen that the maximum amplitude shifts towards the right side in the time axis with the increment of crack size.
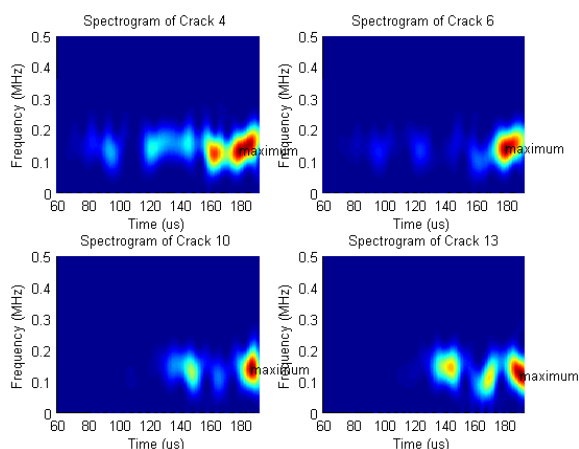

Figure 15   STFT analysis of the four cracks (R1-R5)

5   CONCLUSION

This paper has presented a dual mode sensing approach for crack detection in steel bridge health monitoring using transducers which are traditionally designated for passive AE measurement. Passive AE monitoring can be able to detect crack growth by picking up the stress waves resulting from the breathing of cracks. R15I AE transducer is conventionally used as passive acoustic emission transducer. Our research has shown its high quality in detection and localizing acoustic emission. With their built-in AST option, R15I has the potential of being used as active ultrasonic transducer, being both transmitter and receiver in the interrogation. Hence, the active sensing capability of R15I was also explored. For the active sensing, apparent velocity of wave propagation was introduced to explain the difference between the velocity calculated from the 'without crack pairs' in the pristine specimen and the

velocity calculated from the 'with crack' pair throughout the crack development. It can be concluded that the wave energy is scattered because of the crack; therefore, the calculated wave speed is decreased when the wave propagation path is broken. Additional analyses with damage index, STFT, and filtering have also been explored for further understanding the changes in apparent velocity of wave propagation.

To better understand the wave propagation in the subject specimen, the next step of this research will be utilizing finite element modeling (FEM) approach to simulate the plate waves propagation and interaction with crack in the structure. We will focus on the comparison of the experimental data and the simulation data in order to fully understand the apparent velocity of wave propagation.

6   ACKNOWLEDGMENTS

REFERENCES

1. Pullin, R.; Holford, K.; Lark, R.; Eaton, M. (2008) "Acoustic Emission Monitoring of Bridge Structure in The Field and Laboratory", *Journal of Acoustic Emission*, Vol 26, pp.172-181
2. Nair, A.; Cai, C. (2010) "Acoustic Emission Monitoring of Bridge: Review and Case Studies", *Journal of Engineering Structure*, Vol 32, pp.1704-1714
3. Shiotani, T.; Aggelis, D.; Makishima, O. (2007) "Global Monitoring of Concrete Bridge Using Acoustic Emission", *Jounal of Acoustic Emission*, Vol. 25, pp. 308-315
4. Vahaviolos, S. J. (1996) "Acoustic Emission: A New but Sound NDE Technique and Not A Panacea", *Non-Destructive Testing*, pp.: 101-115
5. Tan, A.C.C.; Kaphle, M.; Thambiratnam, D. (2009) "Structural Health Monitoring of Bridges Using Acoustic Emission Technology", *IEEE Proceedings of the 8th International Conference on Reliability*, Maintainability and Safety, pp. 839-843
6. Grosse, C.U.; Ohtsu, M. (2008) "Acoustic Emission Testing Basics for Research Applications in Cibil Engineering", Leipzig, Germany, Springer
7. Yu, J.; Ziehl, P.; Zaratea, B.; Caicedo, J.; Yu, L.; Giurgiutiu, V.; Matta, F.; Metrovich, B. (2010) "Quantification of Fatigue Cracking in CT Specimens with Passive and Active Piezoelectric Sensing", *Proceeding of 2010 SPIE*, Vol. 7649, pp. 7649-25
8. Yu, L.; Momeni, S.; Godinez, V.; Giurgiutiu, V.; Ziehl, P.; Yu., J. (2012) "Dual Mode Sensing with Low-Profile Piezoelectric Thin Wafer Sensors for Steel Bridge Crack Detection and Diagnosis", *Advances in civil Engineering*, Vol. 2012, pp. 1-10

9. Yu, L.; Giurgiutiu, V. (2009) "Multi-Mode Damage Detection Methods with Piezoelectric Wafer Active Sensors", *Journal of Intelligent Materials Systems and Structures*, Vol. 20, pp. 1329-1341

10. Rose, J.L. (1999) "Ultrasonic Waves in Solid Media", *Cambridge University Press*

11. Cohen, L. (1995); "Time-Frequency Analysis", New Jerse, *Prentice Hall PTR*